True-amplitude common-shot acoustic reverse-time migration

Yilong Qin and Ray McGarry, Acceleware Ltd.*

Summary

Generating true-amplitude acoustic reverse time migration (RTM) shot images is an important step for improving the quality of an RTM image. One way to generate a true-amplitude RTM common-shot image is via Least-Squares RTM (LSRTM). But iterative LSRTM can be computationally expensive. In practice, a cross-correlation imaging condition (CCIC) with source illumination normalization is often used in the conventional time-domain RTM. However, the CCIC with source illumination normalization does not produce a true-amplitude RTM common-shot image, if the directional fold correction factor (or the horizontal slowness at each receiver) is not accounted for while back-propagating the receiver wavefield.

In this paper, enlightened by the true-amplitude Kirchhoff common-shot inversion formula, we propose an approach to generate the true-amplitude RTM common-shot image by incorporating the directional fold correction into the receiver wavefield. Synthetic examples in constant and v(z) models show that, in the absence of low-frequency self-correlation noises, a true-amplitude acoustic RTM common-shot image can be obtained by combining the source-illumination-normalized cross-correlation imaging condition with the directional fold correction factor. Imaging of a modified version of the Marmousi-II model is also shown to demonstrate the effectiveness of our proposed approach.

Introduction

RTM is based on solving the two-way wave equation which carries the correct propagation amplitude and imposes no dip limitation. Thus RTM has the potential capability of migrating multi-arrival reflections, prismatic waves, internal multiples and refractions, provided that the structures responsible for generating these are included in the input model. Therefore, acoustic RTM with a good propagator can generate better images of complex structures kinematically, as seen in the RTM image of the BP 2004 dataset (Etgen et al., 2009). However, for real application to broadband, noisy field datasets such as land datasets, the overall quality of RTM imaging is generally not as good as true-amplitude Kirchhoff Depth Migration (KDM) or true-amplitude one-way wave-equation migration (Zhang et al., 2005; Arntsen et al., 2010).

Generally, the amplitude and quality of a migration image are affected by some common factors such as errors in the velocity model (Jones & Fruehn, 2003), hitcount normalization, compensation for attenuation/transmission losses, data regularization, muting, noise removal and other data pre-conditioning. In addition to these common factors, RTM-specific factors affecting image quality/amplitude include the choice of imaging condition, removal of low-frequency self-correlation noise (e.g. Zhang & Sun, 2009; Guitton et al., 2007) and that RTM is a shot-profile migration. Numerous RTM imaging conditions have been proposed, including the excitation-amplitude/excitation-time imaging condition (Nguyen & McMechan, 2013; Chattopadhyay & McMechan, 2008), inverse scattering imaging condition (Whitmore & Crawley, 2012), impedance kernel imaging condition (Luo et al., 2012), CCIC with receiver illumination normalization (Kaelin et al., 2007) and CCIC normalized by source illumination and scaled by square cosine of reflection angle (Kiyashchenko et al., 2007).

Various efforts to improve the image quality or the amplitude of RTM images have been made, among which are attenuation loss compensation (Suh et al., 2012), transmission loss compensation (Deng & McMechan, 2007), smart stacking (Compton & Stork, 2012; Whiteside et al., 2012), hybrid source and receiver illumination compensation (Kaelin et al., 2007; Du et al., 2012), true-amplitude RTM angle-domain CIG (Zhang et al., 2009; Xu et al., 2011), source/receiver ghost removal (Zhang et al., 2012), hybrid shot-by-shot and global source illumination normalization (Cogan et al., 2011) and least-squares reverse time migration (LSRTM) (Dong et al., 2012; Yao et al., 2012). LSRTM can produce a true-amplitude common-shot image as well as suppress low-frequency noise, stretched wavelets at shallow depths and migration swings, since it poses migration as an inverse, rather than an adjoint, problem. The major disadvantage of LSRTM is its relatively high computational cost. So, in practice, CCIC with source illumination normalization is often used to approximate LSRTM. By taking only the diagonal elements of the simplified Hessian matrix derived under the linearized scattering approximation and then assuming receiver illumination to be constant, LSRTM reduces to the CCIC with source illumination normalization (Plessix & Mulder, 2004; Du et al., 2012).

In recent years, increased emphasis has been placed on ensuring that migrated images or common image gathers are "true-amplitude". For example, Zhang et al. (2007) give true-amplitude migration weighting factors in various domains. We repeat some of these factors in Table 1. In this work we refer to the surface-angle-based migration

weights such as $\frac{\cos(\alpha_{r0})}{v_0}$ as *directional fold correction* factors.

Domain of migration	Migration weight
Common-shot	$\frac{\cos(\alpha_{r0})}{v_0}\frac{A_r}{A_s}$
Common-angle	$\frac{\cos(\alpha_{r0})}{v_0}\frac{\cos(\alpha_{s0})}{v_0}A_rA_s$
Common-offset	$\frac{\cos(\alpha_{s0})}{v_0}\frac{A_s}{A_r}+\frac{\cos(\alpha_{r0})}{v_0}\frac{A_r}{A_s}$

Table 1: 2D true-amplitude migration weights for different migration domains (from Zhang et al., 2007).

A few efforts have been made to assess the amplitude behavior of acoustic RTM shot imaging for different imaging conditions (Chattopadhyay & McMechan, 2008; Schleicher et al., 2008). However, in those studies, the directional fold correction factors were not taken into account. In this study, we will address the effect of directional fold correction, and show that a true-amplitude RTM common-shot image can be obtained by combining the source-illumination-normalized CCIC with the directional fold correction.

True-amplitude acoustic common-shot RTM

The true-amplitude common-shot Kirchhoff inversion formula is (Zhang et al., 2007; Hanitzsch, 1997)

$$R(x,x_s)=\iint i\omega\frac{\cos(\alpha_{r0})}{v_r}\frac{A(\mathbf{x}_r,\mathbf{x};\omega)}{A(\mathbf{x},\mathbf{x}_s;\omega)}e^{i\omega[\tau(\mathbf{x}_r,x)+\tau(x,x_s)]}D(\mathbf{x}_s,\mathbf{x}_r;\omega)d^2\mathbf{x}_r d\omega \quad (1)$$

where $R(x)$ is the reflector map which can be used to estimate the reflection coefficient on the reflector. v_r is the wave speed at the receiver location and α_{r0} is the emergent angle, i.e., the angle between the ray from x_r to x and the downward normal to the acquisition surface. $A(x_r,x)$ and $A(x,x_s)$ are the Green function amplitudes for waves from the source x_s or receivers x_r, respectively, to the imaging point at x . $D(x_s,x_r;\omega)$ is the observed data in the frequency domain. $\tau(x_r,x)$ and $\tau(x,x_s)$ are the traveltimes from receivers x_r, or source x_s, respectively, to the imaging point at x. $i\omega$ is required to pre-condition the input data for counteracting the effects of Huygens summation.

From equation 1, it can be seen that obtaining a true-amplitude common-shot image requires proper account to be taken of (i) the direction fold correction, $\frac{\cos(\alpha_{r0})}{v_r}$, and (ii) the ratio $\frac{A(\mathbf{x}_r,\mathbf{x};\omega)}{A(\mathbf{x},\mathbf{x}_s;\omega)}$ at each frequency component, i.e., the deconvolution imaging condition (Zhang et al., 2005). The deconvolution imaging condition is simple to apply for frequency-domain one-way wave equation migration. However, it is difficult to implement it for time-domain RTM. Based on these 2 observations, we propose the following imaging condition for producing an amplitude-preserved RTM common-shot image

$$R(\boldsymbol{x})=\frac{\int P_U(\boldsymbol{x};\omega)P_D^*(\boldsymbol{x};\omega)d\omega}{\int P_D(\boldsymbol{x};\omega)P_D^*(\boldsymbol{x};\omega)d\omega+\epsilon} \quad (2)$$

Where ϵ is a damping parameter to avoid numerical instability issues when the denominator is too small. $P_D(\boldsymbol{x};\omega)$ is the source wavefield. $P_U(\boldsymbol{x};\omega)$ is the receiver wavefield obtained by back-propagating pre-conditioned shot gathers and is denoted as

$$P_U(\boldsymbol{x};\omega)=\int D(\boldsymbol{x}_r;\omega)G^*(\boldsymbol{x}_r,\boldsymbol{x};\boldsymbol{\omega})\frac{i\omega cos(\alpha_{r0})}{v_r}d^2\boldsymbol{x}_r \quad (3)$$

Where $G^*(\boldsymbol{x}_r,\boldsymbol{x};\boldsymbol{\omega})$ is the complex conjugate of the Green function between receiver $\boldsymbol{x}_r$ and image point $\boldsymbol{x}$. Here, it needs to be pointed out that the directional fold correction factor $\frac{\cos(\alpha_{r0})}{v_r}$ should be incorporated into the back-propagated receiver wavefield, which can be converted into partial differential operators and modifications to initial and/or boundary conditions (Leveille et al., 2011).

The imaging condition shown in equation 2 is an approximation of deconvolution imaging in the least-squares sense by assuming the reflectivity is frequency-independent (Schleicher et al., 2007; Chazalnoel et al., 2012). According to Parseval's theorem, equation 2 can be converted into the time domain, giving

$$R(\boldsymbol{x})=\frac{\int P_U(\boldsymbol{x};t)P_D(\boldsymbol{x};t)dt}{\int P_D(\boldsymbol{x};t)P_D(\boldsymbol{x};t)dt+\epsilon} \quad (4)$$

This is simply the standard cross-correlation imaging condition with source illumination normalization and can be implemented into time-domain RTM efficiently. In the next section, we will generate true-amplitude RTM common-shot images for different models, based on equations 3 and 4.

Numerical examples

To show how the proposed true-amplitude common-shot RTM works, we present here 3 numerical tests in a constant velocity model and a v(z) model, in which the effect of low-frequency self-correlation noise is excluded. Then we show its effect on the stacked image of a modified Marmousi-II model.

Figure 1a shows the true-amplitude common-shot RTM image for a 2D flat density-contrast reflector model with constant velocity of 3000m/s. The input synthetic shot gather is generated by assuming the amplitudes of recorded

reflection events are only affected by geometrical spreading. These 3 reflectors have the same theoretical angle-independent reflectivity. Figure 1b shows the picked peak amplitude along the 3 reflectors of the true-amplitude common-shot image shown in Figure 1a, which matches well with the theoretical reflectivity. As a comparison, the peak amplitude of the shot image without incorporating the directional fold is shown in Figure 1c, where the amplitude of migrated reflectors is overestimated, especially for shallow reflectors illuminated by far-offset traces. However, the error is zero at zero offset, since the emergent angle is zero.

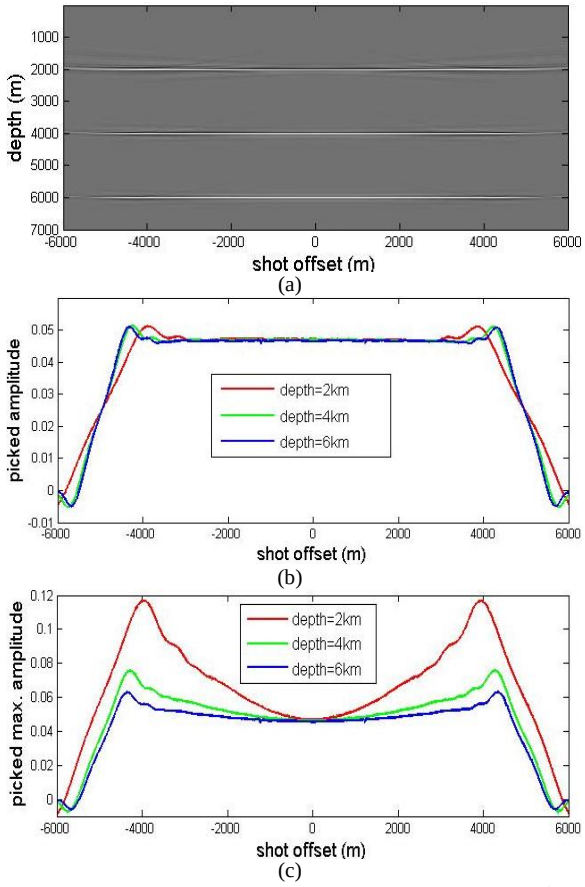

Figure 1: (a) RTM shot image incorporating directional fold correction. The model has 3 horizontal density-contrast reflectors and constant velocity of v=3000m/s. (b) Peak amplitude along the 3 reflectors of shot image (a). (c) Peak amplitude of the shot image without incorporating directional fold correction.

Figure 2 shows a similar example to Figure 1, but for 3 dipping reflectors with the same angle-independent reflectivity. 2 of the dipping reflectors intercept with the acquisition surface. Again, the true-amplitude common-shot RTM produces accurate amplitudes, even for very shallow steep-dipping reflectors, as shown in Figure 2b. Figure 2c shows that, for increasing reflector dip, the directional fold correction has more effect.

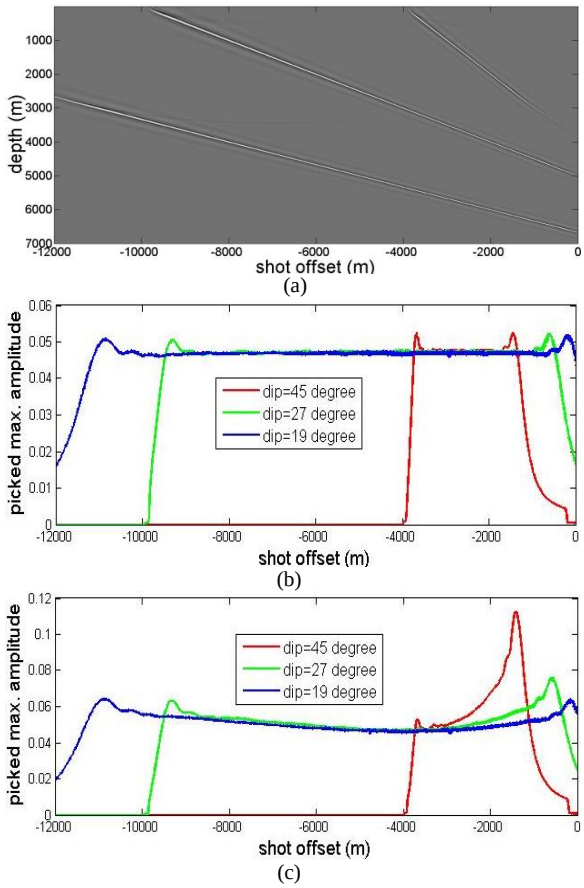

Figure 2: (a) RTM shot image incorporating directional fold correction, for a model with 3 dipping density-contrast reflectors and constant velocity of v=3000m/s; (b) Peak amplitude along the 3 dipping reflectors of shot image (a); (c) Peak amplitude of the shot image without incorporating directional fold correction.

Figure 3 shows a similar example to Figure 2, but for a v(z) model. The input shot gather is generated by using finite-difference acoustic modeling. Direct arrivals are muted before migration. From this test, we can see that the proposed true-amplitude common-shot RTM can recover the reflectivity in a v(z) model accurately. It can also be noted that directional fold correction has less effect in a v(z) model than in a constant velocity model, since the emergent angle will be smaller for the v(z) model.

Finally, we show the stacked image of a modified Marmousi-II model in Figure 4. A total of 300 shots are simulated by using an extract of the Marmousi-II velocity model (Martin et al., 2006), with the water depth reduced to 50m as in the original Marmousi model. A 25Hz Ricker

wavelet is used as the source wavelet. For a single shot record, receivers with a maximum offset of 3km are deployed on the left side of the shot. An absorbing surface boundary condition is used.

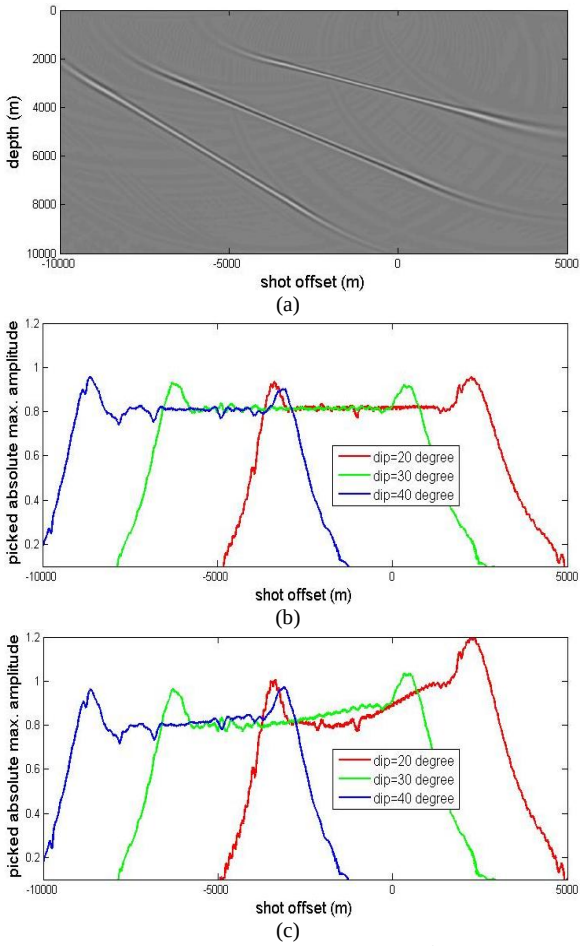

Figure 3: (a) true-amplitude RTM shot image for a v(z) model (v=(2400+0.3z)m/s). The model has 3 dipping density-contrast reflectors with the same theoretical absolute reflectivity; (b) Picked peak amplitude along the 3 dipping reflectors of shot image (a); (c) Picked peak amplitude of the shot image without incorporating directional fold correction.

Figure 4a is the stacked image by using true-amplitude common-shot RTM and a post-imaging filter to remove the RTM low-frequency noise. This shows well-balanced amplitudes compared to the true reflectivity and well-imaged shallow steep dips. As a result of transmission loss, the amplitude of imaged reflectors underneath the complex fault is a bit lower. Figure 4b shows the stacked image without incorporating directional fold correction. The amplitude and phase are very similar to Figure 4a, except for the shallow part. In generating Figures 4a and 4b, no mute is applied to either input shot gathers or shot images. It can be seen that true-amplitude common-shot RTM can improve the image quality of the shallow part significantly.

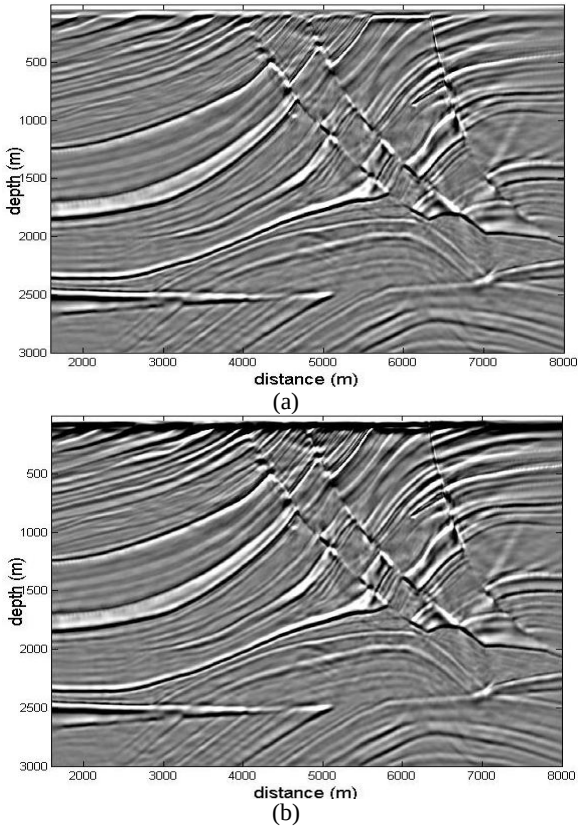

Figure 4: RTM stacked image of modified Marmousi-II model. (a) directional fold is accounted for; (b) directional fold correction is ignored.

Conclusions and discussion

By incorporating the directional fold correction into the back-propagated receiver wavefield, the CCIC with source illumination normalization can produce a true-amplitude RTM common-shot image. The amplitude of imaged events with large reflection angle will be overly estimated if the directional fold correction is ignored. The image quality at shallow depths can be significantly improved by stacking true-amplitude common-shot images without using any spatially-varying mute.

CCIC will generate undesirable low-frequency self-correlation noise in the presence of strong velocity contrasts. This low-frequency noise needs to be removed properly without distorting the amplitude of imaged reflectors.